Journal of Electron Microscopy **51(Supplement)**: S79–S85 (2002)

Full-length paper

Measuring the Young's modulus of solid nanowires by *in situ* TEM

Zhong Lin Wang[1,*], Zu Rong Dai[1], Ruiping Gao[1] and James L. Gole[2]

[1]School of Materials Science and Engineering and [2]School of Physics, Georgia Institute of Technology, Atlanta, GA 30332-0245-0430, USA

*To whom correspondence should be addressed. E-mail: zhong.wang@mse.gatech.edu

Abstract Property measurements of individual nanowires are challenging due to the small sizes of the structures. Scanning probe microscopy has thus far been the dominant tool for the characterization of nanomaterial properties. We have developed an alternative novel approach that allows a direct measurement of the mechanical properties of individual nanowires by *in situ* transmission electron microscopy (TEM). The technique relies on the electric field induced mechanical resonance of the nanowire observed in TEM, as it directly correlates the atomic-scale microstructure of the nanowire with its physical properties. In this paper, the measurement of Young's modulus for composite SiO_2/SiC wires is reported. The experimental results are in agreement with theoretically expected values.

Keywords nanotube, nanowire, *in-situ* TEM, Young's modulus

Received 13 November 2000, accepted 3 July 2001

Introduction

The mechanical properties of nanowires can have important application to the development of composite materials. With their significant size and structural diversity, the physical properties of nanomaterials strongly depend on their atomic-scale structure, their mode of preparation, and the chemistry that they can undergo. To fully utilize this unique regime and the basic and technological advantages offered by the size specificity and selectivity of nanowires, it is essential to investigate the structural characteristics of individual nanowires. Scanning probe microscopy (STM, AFM) has been a powerful tool in manipulating and characterizing the properties of individual nanostructures. Thus far, this technique has provided the dominant approach to nano-scale manipulation [2,3]. Transmission electron microscopy (TEM), on the other hand, has been applied traditionally to the characterization of the internal structures of nanomaterials.

The measurement of the Young's modulus of carbon nanotubes was first carried out using TEM by quantifying the thermal vibration amplitude of the nanotube [4]. Within the framework of *in situ* TEM, recently we have developed a novel approach that relies on electric field induced mechanical resonance for measuring the properties of individual wire-like structures [5–7]. This is a new technique that not only can provide the properties of an individual nanowire but also can give the structure of the nanowire through electron imaging and diffraction. The technique, thus, provides an ideal means for understanding the one-to-one property–structure relationship. In this paper, this *in situ* TEM technique is applied to measuring the mechanical properties of SiO_2/SiC composite nanowires.

Methods

Synthesis of nanowires

The nanowires used for this study are SiO_2/SiC composite nanowires, which are synthesized by a solid–vapour phase reaction process, as reported in detail elsewhere [8,9]. Key to the experiments is that amorphous SiO is brought into intimate contact with carbon/graphite in an appropriate mix at elevated temperatures for an extended time period. This is facilitated as a SiO and carbon mix placed into a low porosity carbon crucible at the centre of a temperature controlled tube furnace, operated with a double concentric alumina tube combination. The appropriate mixture is heated to the desired temperature to form composites as the sample is bathed in an entraining argon flow at a flow rate of 100 sccm. The total pressure in the inner alumina tube ranges from 200 to 300 Torr, controlled by a mechanical pump attached to the inner alumina tube through a downstream water-cooled stainless

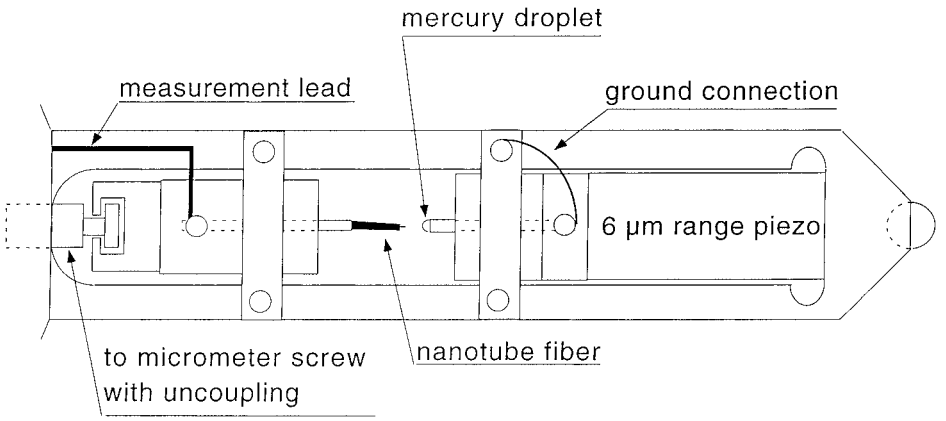

Fig. 1 Schematic diagram of the specimen holder used for *in situ* measurement in TEM.

steel end piece. This end piece is mechanically attached to a 'water cooled' cold plate, whose temperature is adjustable, at the fringes of the tube furnace hot zone. The entrance and exit regions of the alumina tube furnace are insulated by a matching set of zirconia blocks. To produce both coaxial and biaxial silicon carbide–silica nanowire configurations, the system was operated at a temperature of 1500°C for 12 h.

Nanomeasurements by *in situ* TEM

To carry out property measurements on nanowires, a specimen holder for a JEOL 100C TEM (100 kV) was built to facilitate the application of a voltage across a nanowire and its counter electrode (Fig. 1). The specimen holder requires the translation of the nanowire via either mechanical movement by a micrometer or by an exial directional piezo. The fibre was glued using silver paste onto a gold wire, through which an electric contact was made. The counter electrode was a gold ball directly facing the nanowire. The nanowire whose properties are to be measured is imaged directly under TEM, as both electron diffraction patterns and images can be recorded from the nanowire. The information provided by TEM directly reveals both the surface and internal structure of the nanowire. Our experiments were carried out using a JEOL 100C TEM (100 kV). An oscillating voltage with tuneable frequency was applied to the nanowire. Here, a mechanical resonance can be induced in the nanowire if the applied frequency approaches the resonance frequency (Fig. 2). This technique works for either conductive or insulating nanowires.

Theoretically, for a rod with one end hinged and the other free, the resonance frequency is given by [10]

$$f_0 = (\beta^2 / 2\pi)\,(EI / m)^{1/2} / L^2 \qquad (1)$$

where f_0 is the fundamental resonance frequency, $\beta = 1.875$, EI is the flexural rigidity (or bending stiffness), E is the Young's modulus, I is the moment of inertia about a particular axis of the rod, L is the length of the rod, and m is its mass per unit length.

To apply equation (1) in a data analysis, it is vital to identify the true fundamental frequency. In practical experiments, the nanowires are positioned against a counter electrode. Because of the difference between the surface work functions of the

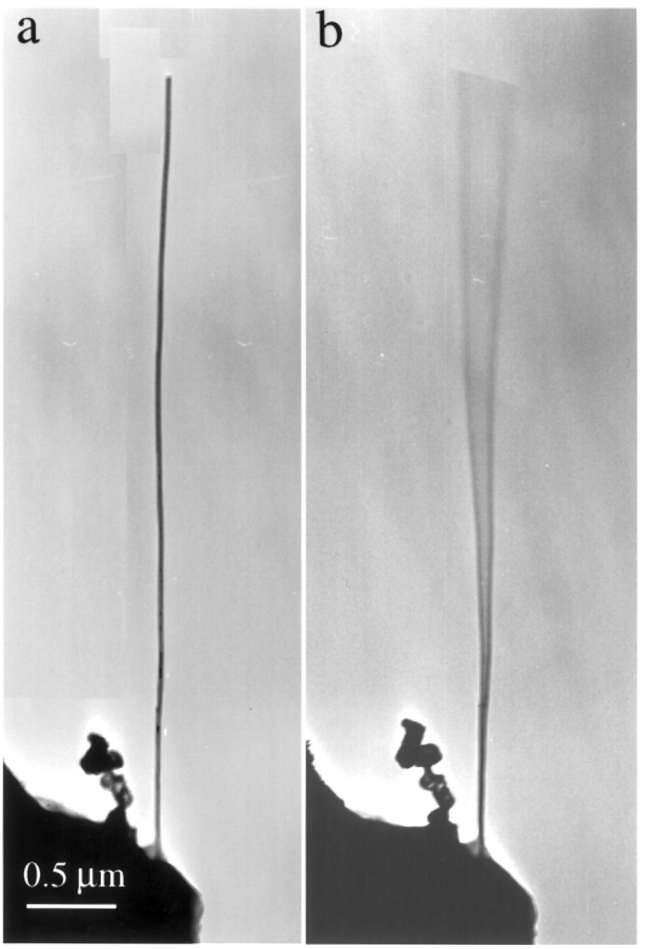

Fig. 2 A silica sheated crystalline silicon or amorphous silica at (a) stationary and (b) the first harmonic resonance induced by an externally applied electric field.

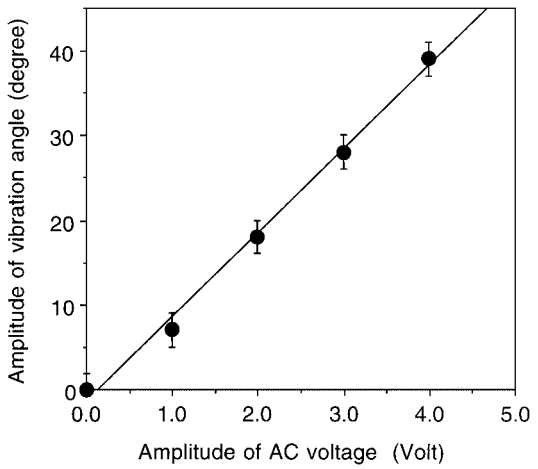

Fig. 3 Experimentally measured full vibration angle of a carbon nanotube as a function of the amplitude of the applied AC voltage.

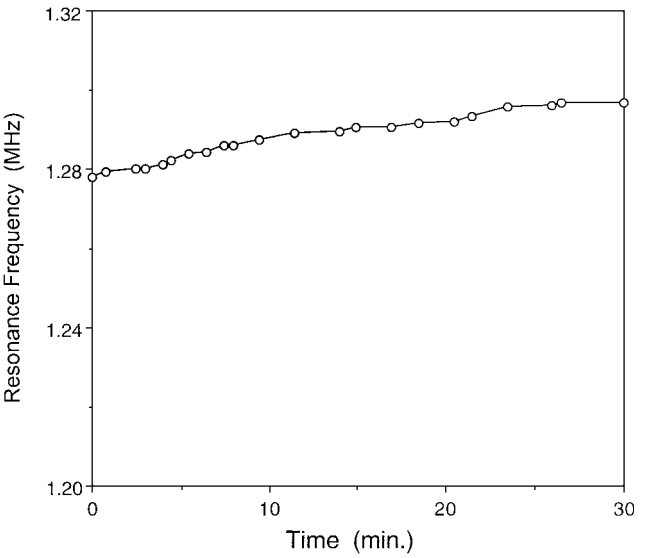

Fig. 4 Time dependence of the resonance frequency of a carbon nanotube being illuminated by 100 kV electrons.

nanowire and the counter electrode (e.g. Au), a static charge exists to balance the potential difference that exists even at zero applied voltage. Therefore, under an applied field the induced charge on the nanowire can be represented by $Q = Q_o + \alpha V_d \cos 2\pi ft$, where Q_o represents the charge on the tip that balances the difference in surface work functions, α is a geometrical factor, and V_d is the amplitude of the applied voltage. The force acting on the nanowire is

$$F = \beta(Q_o + \alpha V_d \cos 2\pi ft)^2 = (\beta Q_o^2 + \alpha^2 \beta V_d^2/2) + 2\alpha\beta Q_o V_d \cos 2\pi ft + \alpha^2 \beta V_d^2/2 \cos 4\pi ft \quad (2)$$

where β is a proportionality constant. Thus, resonance can be induced at f and $2f$ with vibrational amplitudes proportional to V_d and V_d^2, respectively. The former is a linear term, as the resonance frequency equals the applied frequency, while the latter is a non-linear term for which the resonance frequency is twice that of the applied frequency. There are two ways to determine the fundamental frequency. Using the linear relationship, the vibration amplitude is linearly dependent on the magnitude of the voltage V_d (Fig. 3). Alternatively, one needs to examine the resonance at a frequency that is half or close to half of the observed resonance frequency to ensure that no resonance occurs. The latter is the most convenient technique used in practice.

The diameters of nanowires can be determined directly from TEM images with high accuracy. The determination of length requires that we consider the 2-D projection effect of the nanowire. It is essential to tilt the nanowire in order to determine its maximum length (which is likely to be the true length) in TEM. This requires that the TEM be operated at a tilting angle as large as ± 60°. Further, the operation voltage of the TEM must be controlled carefully to minimize radiation damage. The 100 kV TEM used in our experiments produces almost no detectable damage to a nanowire.

To trace the sensitivity of the recorded resonance frequency to electron beam illumination and radiation damage at 100 kV, a carbon nanotube was resonated for more than 30 min. The resonance frequency showed an increase of ~1.4% over the entire period of the experiment (Fig. 4), as no dependence on the electron dose was found. The full width at half maximum (FWHM) for the resonance peak was measured to be $\Delta\nu / \nu = 0.6\%$ in a vacuum of 10^{-4}–10^{-5} Torr. The slight increase in the resonance frequency could be related to a change in nanowire structure under the influence of the electron beam or to the loss of the root end. However, these slight changes cause a negligible effect on the measurement of Young's modulus.

Results

Young's modulus of SiO_x solid nanowires

The as-synthesized materials that we studied are grouped into three basic nanowire structures: pure SiO_x nanowires, coaxial SiO_x sheathed β-SiC nanowires, and biaxial β-SiC/SiO_x nanowires. The Young's modulus was first measured for pure

Table 1. Measured Young's modulus, *E*, for solid silica nanowires. *E* was calculated using the density of bulk amorphous SiO_2

D (nm) (± 2 nm)	*L* (μm) (± 0.2 μm)	f_0 (MHz)	*E* (GPa)
42	11.7	0.160	31 ± 5.1
53	6.3	0.562	20 ± 4.0
58	3.8	1.950	27 ± 7.5
70	13.0	0.200	26 ± 3.1
95	14.8	0.232	32 ± 3.1

f_0, fundamental resonance frequency; *L*, nanowire length; *D*, nanowire diameter.

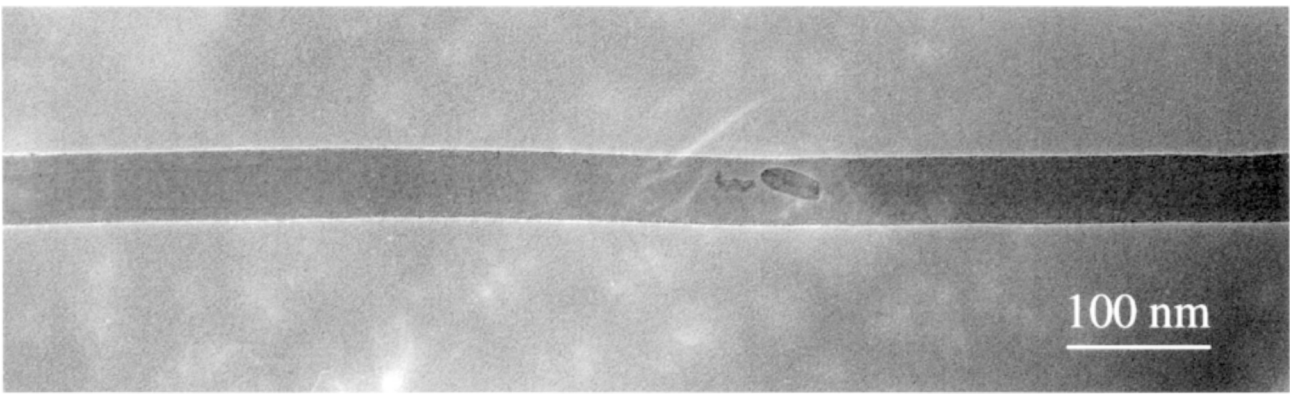

Fig. 5 TEM image of amorphous silica nanowires.

silica nanowires (Fig. 5). From eq. (1), for a uniform solid rod with diameter D, $I = \pi D^4/64$, the Young's modulus is given by

$$E = \rho(8\pi f_0 L^2/\beta^2 D)^2 \quad (3)$$

where ρ is the volume density of the rod. Table 1 catalogues the experimentally measured Young's moduli of silica nanowires. It can be seen that the data are fairly consistent. The Young's modulus for the larger fused silica fibres can be found from the literature: for $D = 102$ μm, $E = 72.3$ GPa; $D = 20$ μm, $E = 71.9$ GPa; and $D = 4.1$–6.0 μm, $E = 56.3$ GPa [11]. Our data suggest modulus about half that of the values for the larger silica fibres. A density of point defects or chemical non-stoichiometry in the wires could account for this difference.

Young's modulus of the coaxial composite nanowires

Coaxial SiO_2 and SiC nanowires are constituted of a cubic structured SiC (β-SiC) core and the SiO_2 sheathed layer (Fig. 6a). High-resolution TEM demonstrates that the wire direction is [111] (Fig. 6c). Cross-sectional TEM images indicate the coaxial structure of the nanowire (Fig. 6b). The core size and the thickness of the sheathed layer are found to vary from wire to wire. For such a coaxially structured nanowire whose core material density is ρ_c and diameter is D_c, and a sheath material density that is ρ_s with outer diameter D_s, the average density of the nanowire can be evaluated from

$$\rho_{\text{eff}} = \rho_c(D_c^2/D_s^2) + \rho_s(1 - D_c^2/D_s^2) \quad (4)$$

If the volume density in eq. (1) is replaced by the effective density given in eq. (4), the effective Young's modulus of the composite nanowire, E_{eff}, is given by

$$E_{\text{eff}} = \rho_{\text{eff}}(8\pi f_0 L^2/\beta^2 D_s)^2 \quad (5)$$

The experimental results are summarized in Table 2, where the Young's modulus is found to increase as the diameter of the nanowire increases. The Young's modulus for the coaxially structured SiC/SiO_x nanowires results from the combination of SiC and SiO_x, where the contribution from the sheath layer of SiO_x exceeds that from the SiC core because of its larger flexural rigidity (or bending stiffness).

To compare the experimentally measured modulus with the theoretically expected modulus, we consider a model in which the coaxial nanowire is taken as a composite material. If we consider that the force that induces the mechanical vibration is closely perpendicular to the axis of the nanowire, from the standard mechanical theory for composites, the Young's modulus of the composite will be given by [12]

$$1/E_{\text{eff}} = V_{\text{SiC}}/E_{\text{SiC}} + V_{\text{Silica}}/E_{\text{Silica}} \quad (6)$$

where $V_{\text{SiC}} = g$ and $V_{\text{Silica}} = 1 - g$, with $g = D_c^2/D_s^2$, are the volume fractions of the SiC core and the silica sheathed layer, respectively, and E_{SiC} and E_{Silica} are the corresponding Young's

Table 2 Measured Young's modulus for coaxially structured SiC/SiO_x nanowires (SiC is the core and silica is the sheath). The densities of SiC and SiO_2 were taken from the bulk values ($\rho_{\text{Silica}} = 2.2 \times 10^3$ kg m^{-3}; $\rho_{\text{SiC}} = 3.2 \times 10^3$ kg m^{-3})

D_s (nm) (± 2 nm)	D_c (nm) (± 1 nm)	L (μm) (± 0.2 μm)	f_0 (MHz)	E_{eff} (GPa) Exp.	E_{eff} (GPa) Theor. (20)
51	12.5	6.8	0.693	46 ± 9.0	73
74	26	7.3	0.953	56 ± 9.2	78
83	33	7.2	1.044	52 ± 8.2	82
132	48	13.5	0.588	78 ± 7.0	79
190	105	19.0	0.419	81 ± 5.1	109

D_s and D_c are the outer and inner diameters of the SiO_x sheath, respectively.

Table 3 Measured Young's modulus for biaxially structured SiC/SiO_x nanowires

D_{wire} (nm) (± 2 nm)	D_{SiC} (nm) (± 1 nm)	L (μm) (± 0.2 μm)	f_0 (MHz)	E_{eff} (GPa) Exp.
58	24	4.3	1.833	54 ± 13.8
70	36	7.9	0.629	53 ± 8.4
83	41	4.3	2.707	61 ± 14.3
92	47	5.7	1.750	64 ± 11.8

D_{wire} and D_{SiC} are the widths across the entire nanowire and across the SiC sub-nanowire, respectively.

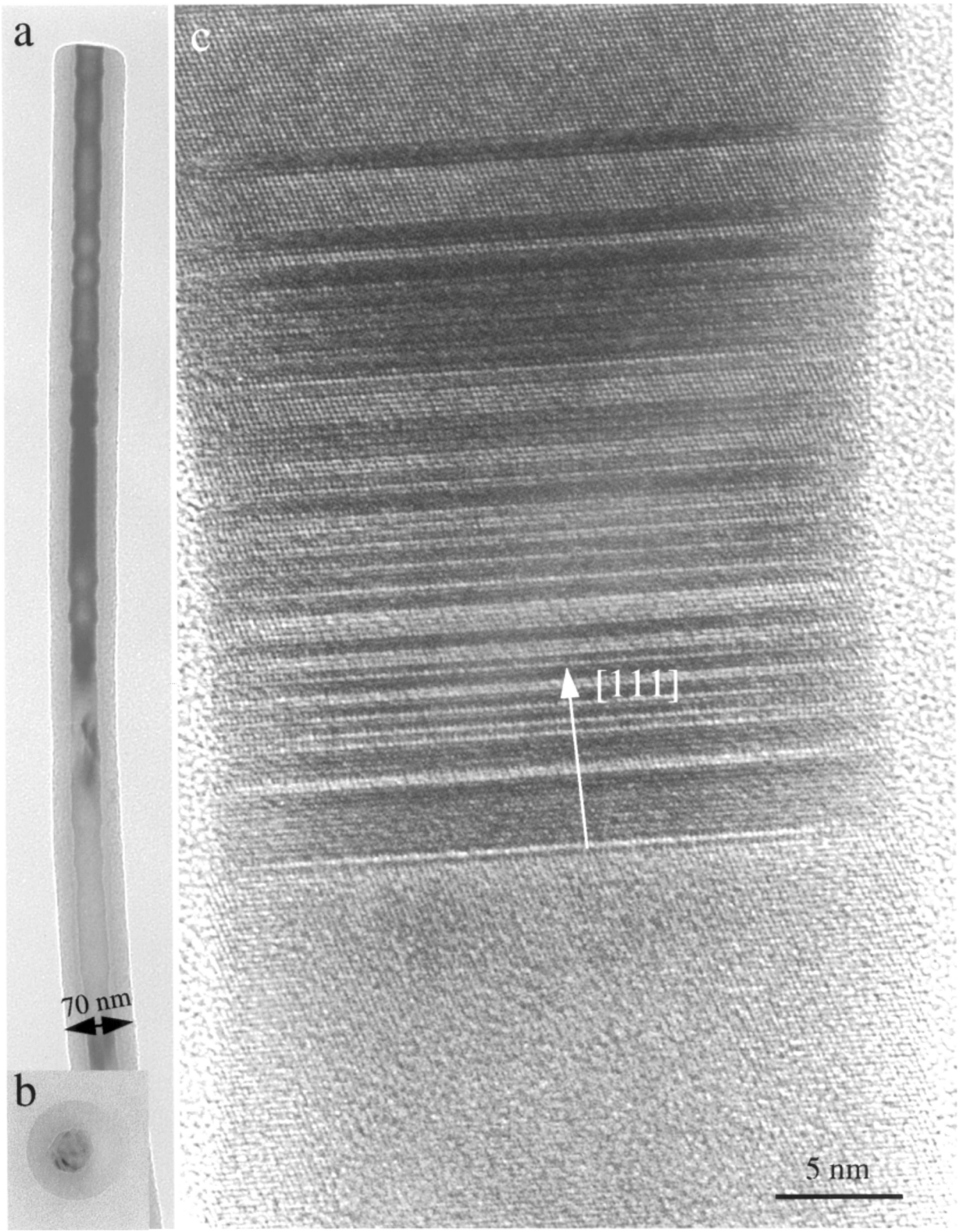

Fig. 6 (a) Low magnification and (b) high-resolution TEM image of a coaxial SiC/SiO_2 nanowire viewed from the side. (c) Cross-sectional TEM image of a coaxial SiO_2/SiC nanowire.

moduli of the bulk materials (E_{SiC} = 466 GPa; E_{Silica} = 73 GPa).

Applying a model, we start with the effective medium theory for a composite rod. The effective flexural rigidity of a composite coaxial nanowire is $E_{eff}I_{eff} = E_{Silica}I_{Silica} + E_{SiC}I_{SiC}$. Thus, the effective Young's modulus of a nanowire with cylindrical symmetry is given by

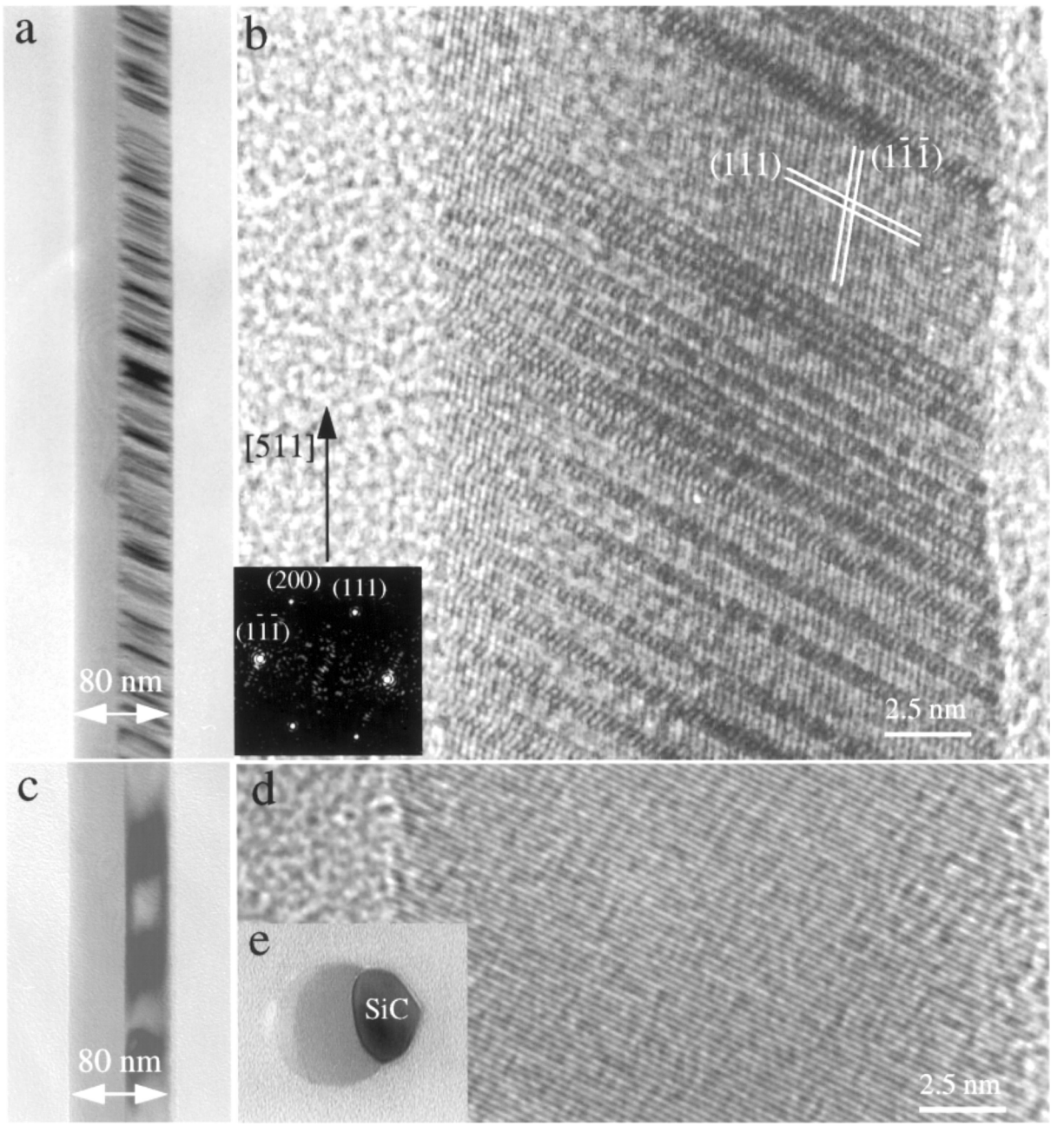

Fig. 7 (a) Low magnification and (b) high-resolution TEM image of a biaxial SiC/SiO_2 nanowire viewed from the side, where the wire has a high density of twins and stacking faults. (c) Low magnification and (d) high-resolution TEM image of a biaxial SiC/SiO_2 nanowire viewed from the side, where the wire is defect free. (e) Cross-sectional TEM image of a biaxial SiO_2/SiC nanowire.

$$E_{\text{eff}} = g^2 E_{\text{SiC}} + (1 - g^2) E_{\text{Silica}} \tag{7}$$

The calculated results from eqs (6) and (7) are listed in Table 2. The determined moduli are both consistent with the measured values. The tendency of the modulus to increase as the diameter increases is in agreement with experimental observation. The data match especially well those values calculated for the larger diameter nanowires.

Young's modulus of the biaxial composite nanowires

Biaxial nanowires consisting of SiC and SiO_2 (Fig. 7a) have also been synthesized [13]. The SiC side would appear to have a high density of microtwins and stacking faults (Fig. 7b), as the growth direction could be [511] or [311] depending on the density of these stacking faults. Biaxial nanowires without stacking faults or twins also are found to grow along [211] (Figs 7c and 7d), but they are rare. The biaxial structure is demonstrated by the cross-sectional TEM image (Fig. 7e), from which the outermost contour of the cross-section of the

nanowire can be approximated to be elliptical. For an elliptical cross-section of half long-axis a and half short-axis b, the moments of inertia are $I_x = \pi ab^3 / 4$ and $I_y = \pi ba^3 / 4$, where a and b can be calculated from the widths of the composite nanowire [10]. With consideration of the equal probability for resonance with respect to either the x or y axes, the effective moment of inertia introduced in calculation is taken to be approximately $I = (I_x + I_y) / 2$. The density per unit length is $m_{\text{eff}} = A_{\text{SiC}}\rho_{\text{SiC}} + A_{\text{Silica}}\rho_{\text{Silica}}$, where A_{SiC} and A_{Silica} are the cross-sectional areas of the SiC and SiO_x sides, respectively. Thus, the effective Young's modulus of the nanowire can be calculated using the formula for a uniform rod with the introduction of an effective moment of inertia and density. The experimentally measured Young's modulus is given in Table 3.

Concluding remarks

The *in situ* TEM approach demonstrated here is unique for measurements of the mechanical properties of wire-like nanomaterials. The properties measured for a single nanowire can be correlated directly with its internal atomic-scale microstructure, providing one-to-one correspondence in the property–structure relationship. The technique relies on the resonance frequency rather than the amplitude, so that the data are recorded with much higher precision. The technique can be applied to any nanowire, either conductive or insulating, provided that the wire is of sufficient length to give a visible vibration that can be observed using TEM.

In addition to the mechanical property measurements reported here, we have applied the technique to observe directly the ballistic electrical transport in a single multiwalled carbon nanotube [14], the results indicating quantum conductance at room temperature [15], and the work-function at the tip of carbon nanotubes [16]. Electron field emission from a single carbon nanotube has been observed also [17]. The technique applies to one-dimensional wire-like structures, such as semiconductor nanobelts [18].

Acknowledgements

We acknowledge the financial support of NSF grant DMR-9733160. Thanks to Prof. Walt de Heer and Dr P. Poncharal for many stimulating discussions. We thank the Georgia Tech Electron Microscopy Center for providing the research facility.

References

1 Wang Z L (1999) *Characterization of Nanophase Materials*. (Wiley-VCH, New York.)

2 Wong E W, Sheehan P E, and Lieber C M (1997) Nanobeam mechanics: elasticity, strength, and toughness of nanorods and nanotubes. *Science* **277**: 1971–1975.

3 Salvetat J P, Briggs G A D, Bonard J M, Bacsa R R, Kulik A J, Stockli T, Burnham N A, and Forro L (1999) Elastic and shear moduli of single-walled carbon nanotube ropes. *Phys. Rev. Lett*. **82**: 944–947.

4 Treacy M M J, Ebbesen T W, and Gibson J M (1996) Exceptionally high Young's modulus observed for individual carbon nanotubes. *Nature* **381**: 678–680.

5 Poncharal P, Wang Z L, Ugarte D, and de Heer W A (1999) Electrostatic deflections and electromechanical resonances of carbon nanotubes. *Science* **283**: 1513–1516.

6 Wang Z L, Poncharal P, and de Heer W A (2000) Nanomeasurements of individual carbon nanotubes by *in situ* TEM. *Pure Appl. Chem*. **72**: 209–219.

7 Gao R P, Wang Z L, Bai Z G, de Heer W A, Dai LM, and Gao M (2000) Nanomechanics of individual carbon nanotubes from pyrolytically grown arrays. *Phys. Rev. Lett*. **85**: 622–625.

8 Lee S T, Zhang Y F, Wang N, Tang Y H, Bello I, Lee C S, and Chung Y W (1999) Semiconductor nanowires from oxides. *J. Mat. Res*. **14**: 4503–4507.

9 Gole J L, Stout J D, Rauch W L, and Wang Z L (2000) Direct synthesis of silicon nanowires, silica nanospheres, and wire-like nanosphere agglomerates. *Appl. Phys. Lett*. **76**: 2346–2348.

10 Meirovich L (1986) *Elements of Vibration Analysis*. (McGraw Hill, New York.)

11 Fisher D J (1990) *Mechanical and Corrosion Properties: Nonmetals*, p. 84, Table 35. (Trans Tech.)

12 Schaffer J P, Saxena A, Antolovich S D, and Sanders T H (1999) *The Science and Design of Engineering Materials*. (McGraw Hill, New York.)

13 Wang Z L, Dai Z R, Bai Z G, Gao R P, and Gole J L (2000) Side-by-side silicon carbide–silica biaxial nanowires: synthesis, structure and mechanical properties. *Appl. Phys. Lett*. **77**: 3349–3351.

14 Poncharal P, Wang Z L, Bai Z G, Keghelian P, and de Heer W A (2000) Are multiwalled carbon nanotubes ballistic conductors? *Phys. Rev. Lett*. (submitted).

15 Frank S, Poncharal P, Wang Z L, and de Heer W A (1998) Carbon nanotube quantum resistors. *Science* **280**: 1744–1746.

16 Gao R P, Pan Z W, and Wang Z L (2001) Work function at the tips of multi-walled carbon nanotubes. *Appl. Phys. Lett*. **78**: 1757–1759.

17 Wang Z L, Poncharal P, and de Heer W A (2000) Nanomeasurements in transmission electron microscopy. *Microsc. Microanal*. **6**: 224–230.

18 Pan Z W, Dai Z R, and Wang Z L (2001) Nanobelts of semiconducting oxides. *Science* **291**: 1947–1949.